

Supplementary Information

Impact of RAFT Chain Transfer Agents on the Polymeric Shell Density of Magneto-Fluorescent Nanoparticles and Their Cellular Uptake

Thibaut Blondy,^a Julien Poly,^b Camille Linot,^a Joanna Boucard,^{a,c} Emilie Allard-Vannier,^d Steven Nedellec,^e Phillipe Hulin,^e Céline Héroumont,^f Lionel Larbanoix,^g Robert N. Muller,^f Sophie Laurent,^{f,g} Eléna Ishow^c and Christophe Blanquart*^a*

^a Nantes Université, Univ Angers, INSERM, CNRS, CRCI2NA, F-44000 Nantes, France.

^b IS2M-UMR CNRS 7361, Université de Haute Alsace, 15 rue Jean Starcky, 68057 Mulhouse, France.

^c Nantes Université, CNRS, CEISAM, UMR 6230, F-44000 Nantes, France.

^d EA 6295 'Nanomédicaments et Nanosondes', Université de Tours, Tours, F-37200, France.

^e Nantes Université, INSERM, UMS 016, CNRS, UMS 3556, F-44000 Nantes, France.

^f Department of General, Organic, and Biomedical Chemistry, NMR and Molecular Imaging Laboratory, University of Mons-Hainaut, B-7000 Mons, Belgium.

^g Center for Microscopy and Molecular Imaging, 8 rue Adrienne Bolland à Gosselies, 6041 Gosselies, Belgium.

OUTLINE	Page
1. UV-vis absorption spectra (<i>Fig. S1</i>)	S2
2. Colloidal stability (<i>Fig. S2-Table S1</i>)	S3
3. ¹ H HR-MAS NMR spectra and monomer ratio analyses (<i>Fig. S3-S5</i>)	S4
4. NA-P3 toxicity (<i>Fig. S6</i>)	S8
5. Internalization of NAs by cell lines cultured in 3D (<i>Fig. S7-S8</i>)	S9
6. Phenotypic characterization of macrophages (<i>Fig. S9</i>)	S11
7. Internalization of NAs by primary mesothelial cells (<i>Fig. S10</i>)	S12

1. UV-VIS ABSORPTION SPECTRA

From the recorded spectra of **P_x** solutions in water, one clearly sees a narrow absorption band centered at 310 nm for **P₂** and a much broader band centered at 300 nm for **P₃** that are typical for $\pi\pi^*$ transitions (Figure S1). The bands related to the much weaker $n\pi^*$ transitions can be distinguished as a shoulder at 445 nm for **P₂** and as a band centered at 499 nm for **P₃**, which accounts for the mentioned pale yellow and pink colors of **P₂** and **P₃** colors respectively. These absorption bands are missing for polyacrylic **P₁** while PEG absorb below 200 nm. Interestingly, given the quite intense and fine absorption band characteristic of the trithiocarbonate group in **P₂**, this band could again be detected on the absorption spectrum of the nanoassemblies **NA-P₂** (see manuscript - Figure 3), thereby demonstrating the presence of the alkyl end groups. For **NA-P₃**, the flatter band makes the detection more tedious.

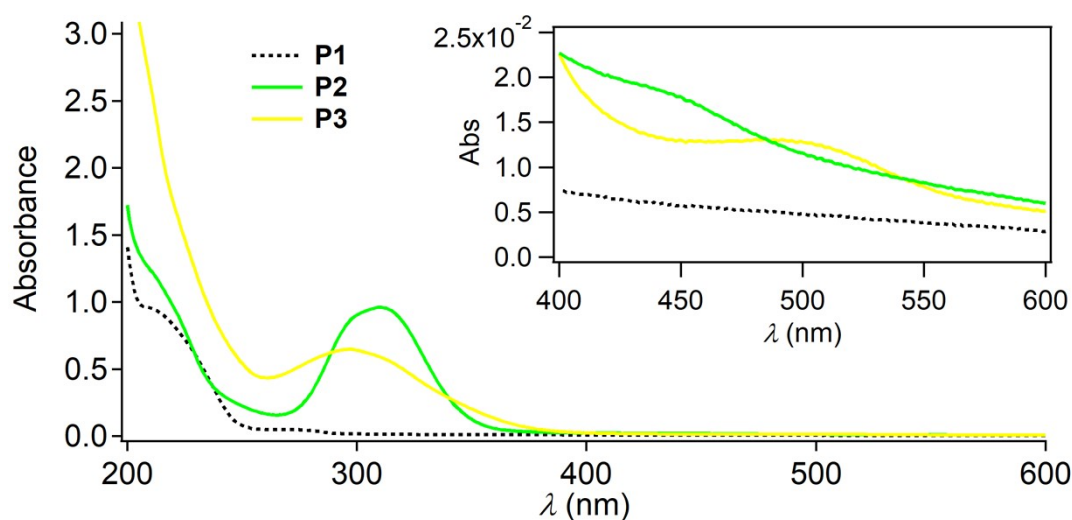


Fig. S1 UV-vis absorption spectra of **P_x** dissolved in water (2 mg **P₁**, 11 mg **P₂** and **P₃**). Inset: zoom-in on the [400-600] nm range.

2. COLLOIDAL STABILITY IN VARIOUS MEDIA

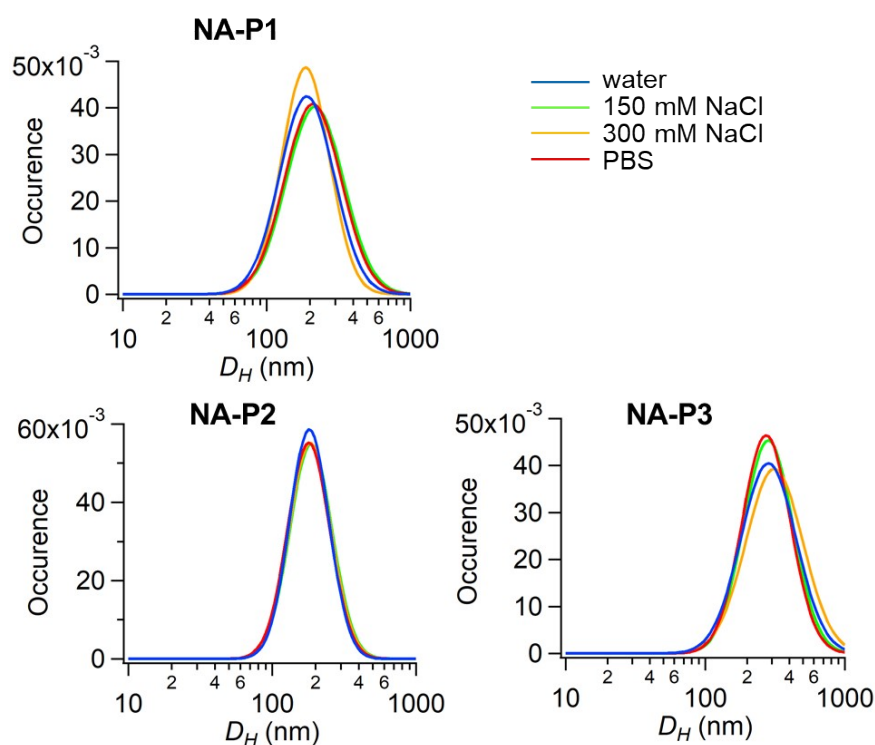


Fig. S2 Size distribution measured by DLS of **NA-P_x** ($x = 1,2,3$) in Millipore water, 150 mM NaCl, 300 mM NaCl, and PBS after at least 30 min equilibration at room temperature.

Table S1. Intensity Z -averaged hydrodynamic diameter D_Z , standard deviation σ , and polydispersity index PDI of **NA-P_x** ($x = 1,2,3$) dispersed in various media (Millipore water, 150 mM NaCl, 300 mM NaCl, and PBS) after at least 30 min equilibration at room temperature, calculated from DLS measurements and considering Cumulants analysis.

	NA-P1		NA-P2		NA-P3	
	$D_Z \pm \sigma$ (nm)	PDI	$D_Z \pm \sigma$ (nm)	PDI	$D_Z \pm \sigma$ (nm)	PDI
water	154 ± 70	0.207	156 ± 50	0.104	208 ± 100	0.231
NaCl 150 mM	158 ± 76	0.233	157 ± 54	0.119	221 ± 94	0.180
NaCl 300 mM	151 ± 59	0.154	155 ± 53	0.118	224 ± 111	0.247
PBS	154 ± 73	0.226	151 ± 52	0.118	216 ± 89	0.171

3. ^1H HR-MAS NMR spectra

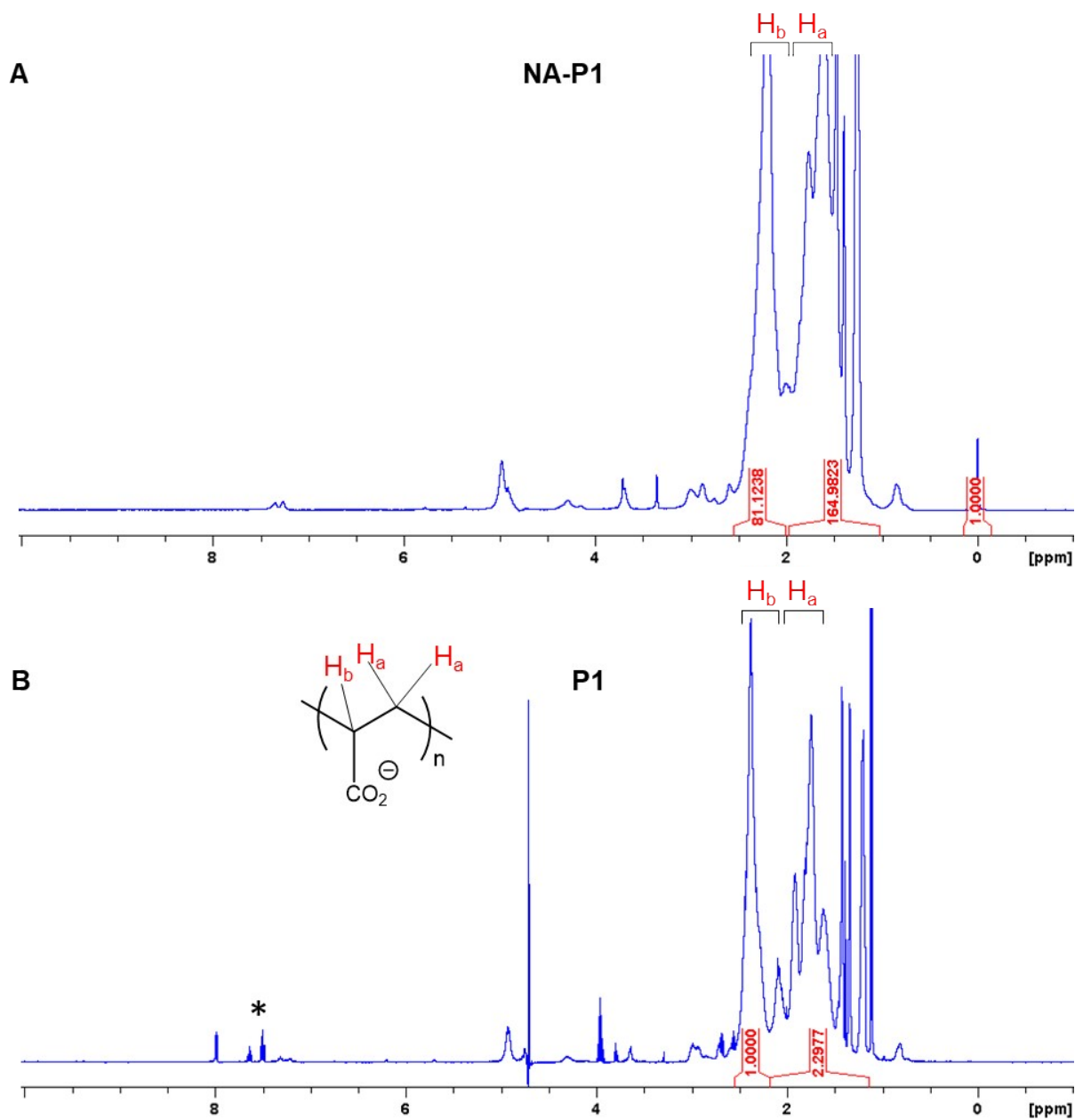


Fig. S3 ^1H HR-MAS NMR spectra recorded at 50 MHz with the noesypr1d sequence of: A) NA-P1, and B) P1 dissolved in D_2O . TSP in a known amount was introduced in the NA-P1 sample for quantification purposes.

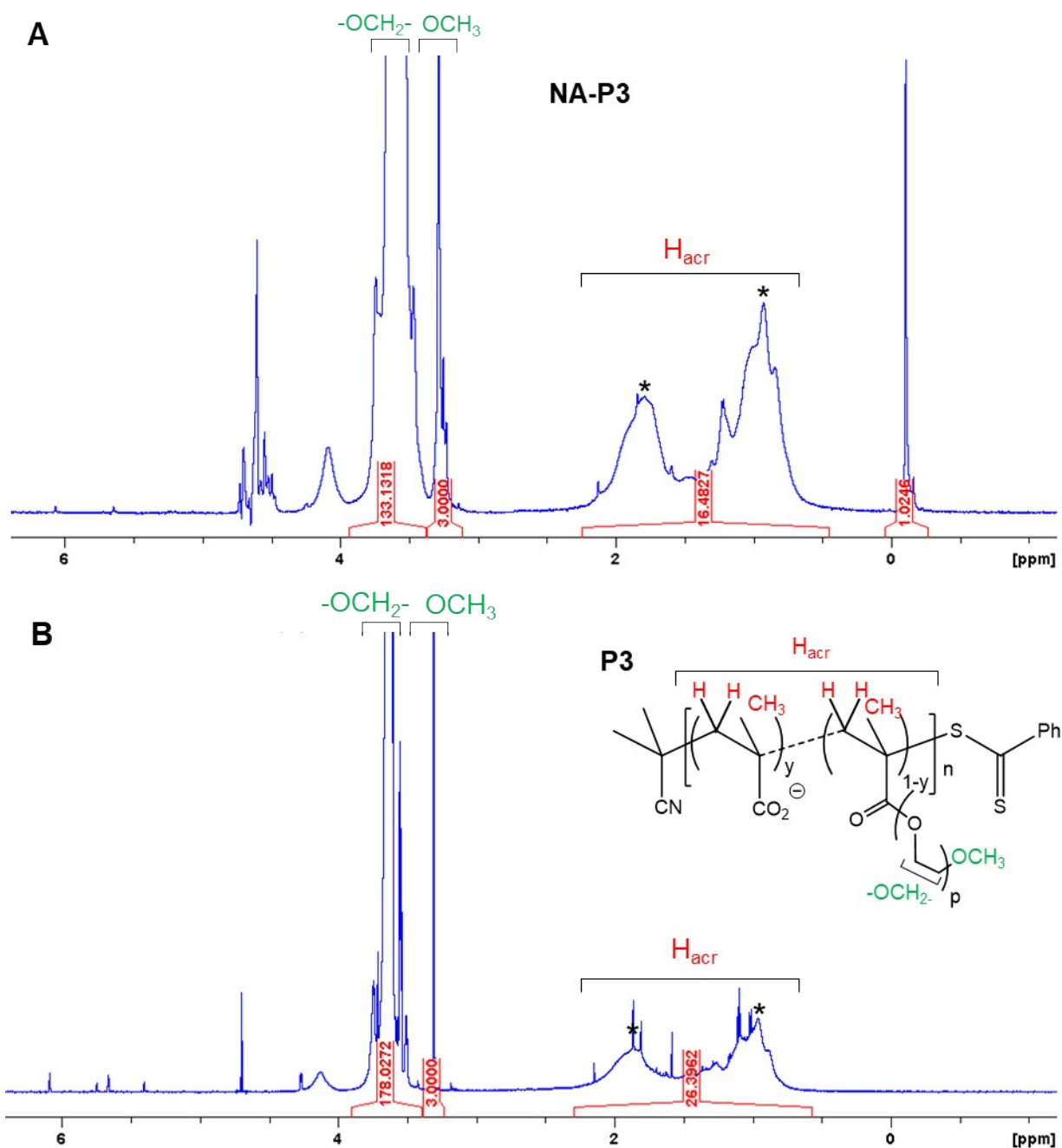


Fig. S5 ^1H HR-MAS NMR spectra recorded at 50 MHz with the noesypr1d sequence of: A) **NA-P3**, and B) **P3** dissolved in D_2O . TSP in a known amount was introduced in the **NA-P3** sample for quantification purposes. The peaks undergoing a +0.8 ppm downfield shift upon **P3** chelation by the iron oxide shell of the nanoparticle surface are indicated with an asterisk.

A fixed integration of 3 protons for the methoxy OCH_3 was chosen to better point out the comparative evolution undergone by **P2** and **P3** upon complexation at the NA surface, and avoid dependence on the known TSP mass introduced in each sample tube.

Monomer ratio analyses by ^1H NMR spectroscopy

The respective ratio of MAPEG against MAA monomers could be calculated from ^1H NMR spectra by integrating the $-\text{OMe}$ signal (3H expected) and $-(\text{OCH}_2\text{CH}_2)-$ signal of the poly(ethylene glycol) chain comprising 43 ethylenoxy moieties (172H expected), and the total protons of the methacrylate chains (5H for each methacrylate unit) which is the number of protons issued from both MAPEG and MAA monomers (150H or 125H expected for **P2** ($n = 30$ units) and **P3** ($n = 25$ units) respectively). We finally found for both polymers the following experimental results that fully agree with the theoretical ones for **P3** and slightly differ by one unit of PEG for **P2**, which may be due to a slight shift from the targeted number n of total units in the methacrylate chains. Nevertheless, this slight difference cannot be responsible for the considerable difference between **P2** et **P3** in terms of photophysics, HR-MAS ^1H NMR spectra and cellular uptake especially in macrophages. It has also no impact on the interpretation of HR-MAS ^1H NMR experiments and calculations of the average density of polymers since we consider relative integration within the same polymer between **P x** and **NP x** ($x = 2,3$) and the final molecular weight issued from GPC analyses.

The reason why we targeted 30 units for **P2** was related to a former study (C. Linot et al., *ACS Appl. Mater. Interfaces* **2017**, *9*, 14242-14257), where the comparative behaviors of non-RAFT and RAFT pegylated polymers based on the same number of methacrylate units, namely 30, were investigated. The particular behavior of **P2** prompted us to question the influence of the RAFT chain end. By changing the number of the new pegylated polymer **P3** to 25 units, close to that of **P1**, we still found that **P2** exhibited a peculiar behavior that could not be related to the length of the polymethacrylate main chain.

Number of MAPEG units per chain	From OMe integration		From $-(\text{OCH}_2\text{CH}_2)-$ integration	
	theoretical	^1H NMR	theoretical	^1H NMR
P2	6	5.04	6	4.98
P3	5	5.28	5	5.10

4. NA-P3 TOXICITY

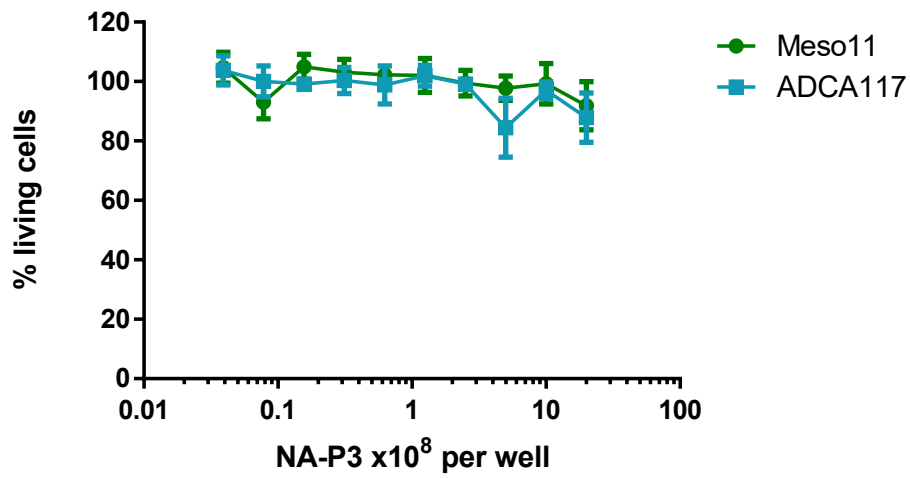


Fig. S6 Evaluation of toxicity of NA-P3. Meso11 and meso34 cells were incubated with increasing amounts of NA-P3 for 72 h. Then, cell viability was evaluated using a CellTiter Glo[®] kit (Promega, Charbonnières-les-Bains, France). Graphics represent means +/- SEM obtained from three independent experiments.

5. INTERNALIZATION OF NAS BY CELL LINES CULTURED IN 3D

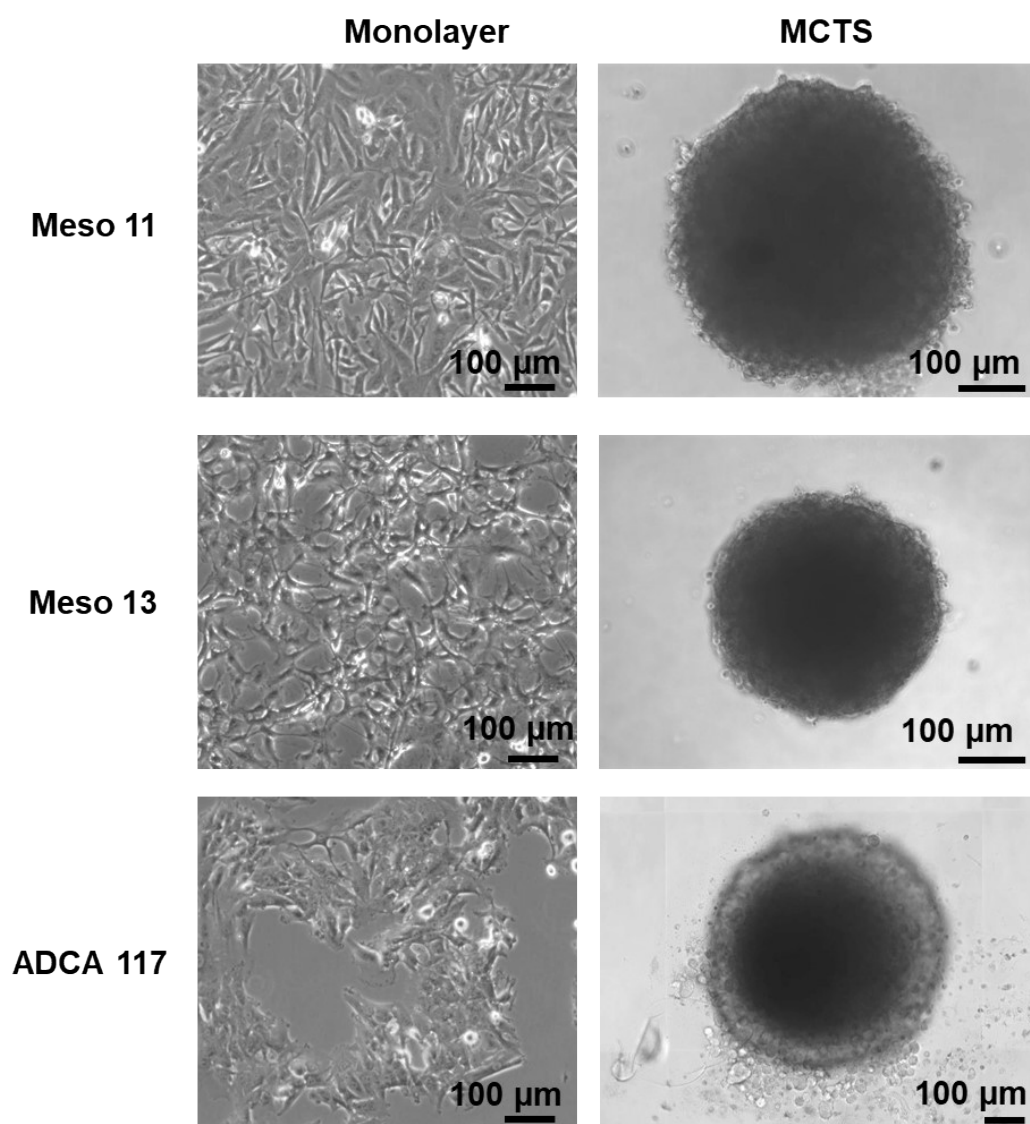


Fig. S7 Transmission imaging of Meso 11, Meso 13 and ADCA 117 cancer cells forming a monolayer or assembled to form MCTS.

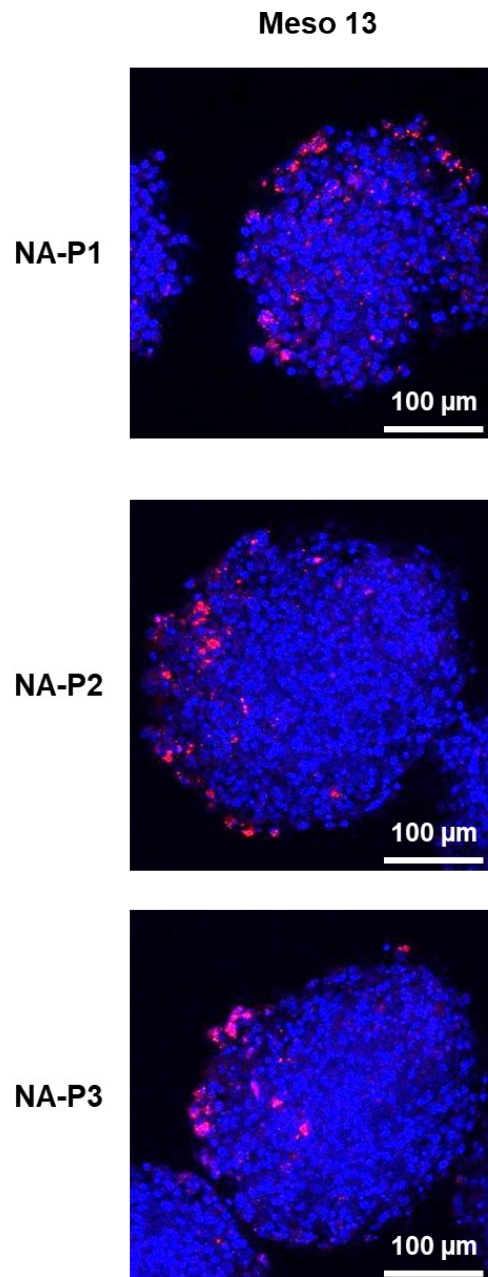


Fig. S8 Confocal fluorescence imaging of Meso 13 cells cultured as MCTS, and incubated with **NA-P1**, **NA-P2** and **NA-P3** for 24 h. Blue: nuclei, pink: NAs.

6. PHENOTYPIC CHARACTERIZATION OF MACROPHAGES

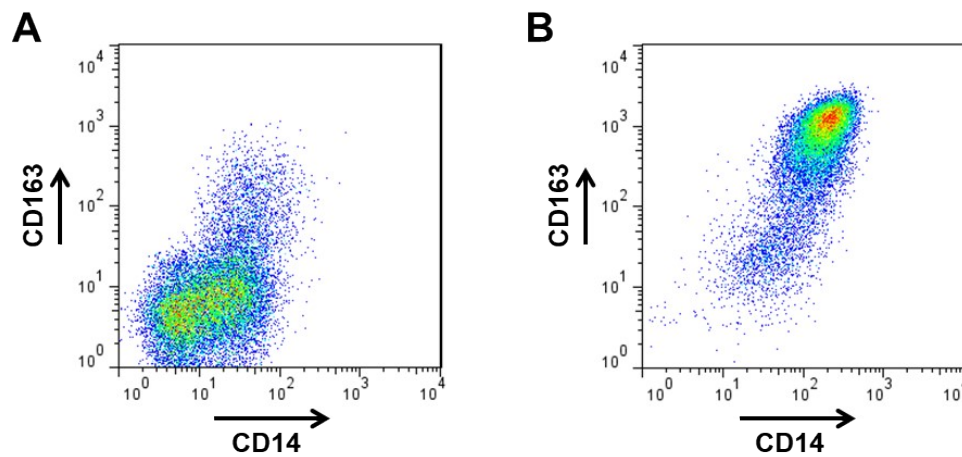


Fig. S9 Phenotypic characterization of macrophages. Macrophages phenotype was studied by flow cytometry using CD14 and CD163 labelling. A) M1-like macrophages characterization. B) M2-like macrophages characterization.

7. INTERNALIZATION OF NAs BY PRIMARY MESOTHELIAL CELLS

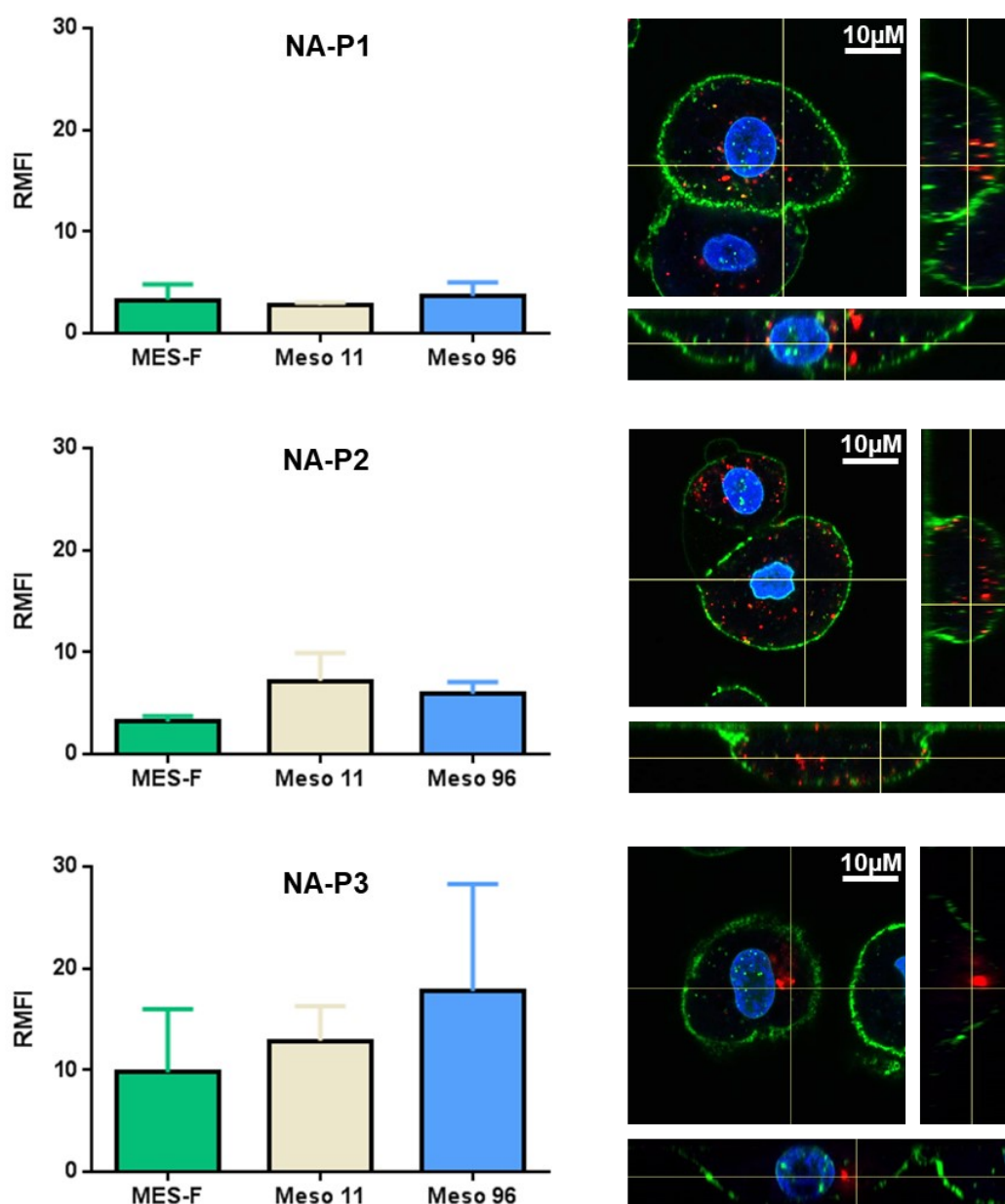


Fig. S10 Internalization of NAs by primary mesothelial cells. Primary mesothelial cells and two MPM cell lines (Meso 11 and Meso 96) were incubated with **NA-P1**, **NA-P2** and **NA-P3** for 24 h. Internalization of the nanoassemblies was studied using flow cytometry (left) and confocal fluorescence microscopy (right).